

Fluorescence and absorption properties of a driven Λ -system

I. V. Bargatin, B. A. Grishanin, and V. N. Zadkov

Faculty of Physics and International Laser Center, M. V. Lomonosov Moscow State University
Moscow 119899, Russia

ABSTRACT

Our investigation is focused on obtaining analytical results describing the resonance fluorescence and weak probe absorption spectra of a driven Λ -system under the Raman resonance condition. For the saturating field limit and within the rotating wave approximation (RWA) the resonance fluorescence and weak probe absorption spectra are calculated for the case of unequal driving fields strengths and non-zero one-photon detunings, generalizing the previously known results.¹ A novel contribution derived is the non-positive non-lorentzian part of the spectrum, originating from the specific quantum properties of the atomic correlation functions. This contribution is asymptotically small under given conditions and, therefore, determines behavior of the resonance fluorescence spectrum wings and the absorption spectrum in the vicinities of the driving fields frequencies. Beyond the RWA, the spectral structures due to the off-resonant four-photon atomic excitations are calculated. They consist of a coherent and two broadened spectral lines centered at the four-photon frequencies $2\omega_L - \omega'_L$ and $2\omega'_L - \omega_L$, respectively, where ω_L and ω'_L are the driving laser frequencies.

Keywords: Coherent population trapping, dark resonance, fluorescence and absorption in Λ -system

1. INTRODUCTION

The resonance fluorescence and weak probe absorption spectra provide a detailed information about internal dynamics of an excited atomic system. Positions of the spectral lines in these spectra are determined by the eigenvalues of the dynamic Liouvillian, i.e., the characteristic frequencies of the system's internal dynamics, while their intensities are strongly dependent on the structure of the eigenvectors of the Liouvillian. This sensitivity of the spectroscopic properties of an atomic system has once provided one of the most precise corroborations of the quantum theory of light-atom interaction.^{2,3}

In theory, we can relatively easy calculate spectroscopic properties of a two-level atom (TLA) and analytical results were published almost for any set of parameters in the literature.^{2,3} Similar calculations for a multi-level atom prove to be much more complicated, making the derivation of the analytical results almost infeasible. Three-level atoms, being an intermediate case between the TLA and multilevel atoms, allow an analytic insight, thus helping us to understand the behavior of more complicated systems. One of the most intriguing effects in the three-level case is the coherent population trapping (CPT), which is most conspicuous in the Λ -system (Fig. 1), when the only transitions between the upper and each of the lower levels are allowed in the dipole approximation.⁴ Under the

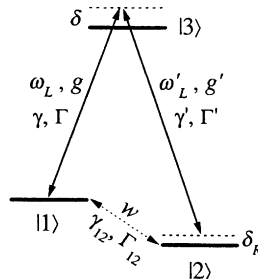


Figure 1. Parameters of a Λ -system driven by two laser fields with the frequencies ω_L and ω'_L . γ , γ' , and γ_{12} are the population decay rates, Γ , Γ' , and Γ_{12} are the dephasing rates, and w is the incoherent pumping rate to the level $|1\rangle$.

Raman resonance condition the total population of the system is trapped in the coherent superposition of the two lower levels, which does not interact with the driving fields. The fluorescence and absorption in the system are strongly suppressed in this case, which gives rise to another name of this phenomenon, the dark resonance.

In this paper, we derive analytical formulae, describing the resonance fluorescence and weak probe absorption spectra for the case of unequal driving fields strengths and non-zero one-photon detunings, which are general case of the previously published results.^{1,5,6} We investigate also a novel contribution to the spectrum, that is the non-lorentzian dispersive part of the spectrum, which appears as we introduce a first order correction in the approximation of the saturating field limit. This contribution despite its asymptotically small value under the given conditions determines the behavior of the spectral intensity of the fluorescence for large frequency offsets, changing drastically the usual lorentzian dependence $\mathcal{F} \propto 1/\Delta\omega^2$ to a more drastic $\mathcal{F} \propto 1/\Delta\omega^4$ in the absence of the inhomogeneous broadening. Dependence of the weak probe absorption in the vicinities of the driving fields frequencies also takes a consistent form as the lorentzian and non-lorentzian parts compensate one another so that the total absorption vanishes, which reflects the CPT in the system.

We calculate also in the first order correction to the rotating wave approximation (RWA) the spectral structure of the four-photon fluorescence, that appears at the four-photon laser frequencies $2\omega_L - \omega'_L$ and $2\omega'_L - \omega_L$, respectively (Fig. 2). These contributions have the same structure as the oscillations in the RF-range, corresponding to the transition between the two lower levels, but is more easily observed in the optical range of frequencies. We show that the four-photon fluorescence spectrum structures consist each of one coherent and up to five (under resonance conditions) broadened lines. Its intensity is lower than the RWA fluorescence spectrum intensity by factor of $g_\Lambda^2 \gamma / \Gamma_{12} \omega_{12}^2$, where $g_\Lambda = \sqrt{g^2 + g'^2}$ is the generalized Rabi frequency and g, g' are the Rabi frequencies of the driving fields.

2. LIOUVILLIAN OF THE DRIVEN Λ -SYSTEM

Hamiltonian of the driven Λ -system is given by (we assume that level $|1\rangle$ has zero energy):

$$\hat{H} = -\hbar\omega_{12} |2\rangle\langle 2| + \hbar\omega_{13} |3\rangle\langle 3| + \hbar g \cos(\omega_L t + \varphi) |1\rangle\langle 3| + \hbar g' \cos(\omega'_L t + \varphi') |2\rangle\langle 3| + \text{h. c.}, \quad (1)$$

where the Rabi frequencies of the driving fields are expressed in terms of the fields amplitudes, $\vec{A}_{\omega_L}, \vec{A}_{\omega'_L}$, and dipole transition matrix elements, $\vec{d}_{13}, \vec{d}_{23}$, as: $g = \frac{1}{\hbar} \vec{d}_{13} \vec{A}_{\omega_L}$ and $g' = \frac{1}{\hbar} \vec{d}_{23} \vec{A}_{\omega'_L}$, respectively. In the interaction picture, with the transformation $\mathcal{U}_0(t) = \exp\left[-(i/\hbar)\hat{\mathcal{H}}_0 t\right]$, where $\hat{\mathcal{H}}_0 = \hbar\omega_L |3\rangle\langle 3| - \hbar\Delta |2\rangle\langle 2|$, and in the RWA the Hamiltonian takes the form:

$$\hat{\mathcal{H}}_\Lambda = \hbar \left[-\delta |3\rangle\langle 3| + \delta_R |2\rangle\langle 2| + \frac{g}{2} |1\rangle\langle 3| + \frac{g'}{2} |2\rangle\langle 3| + \text{h. c.} \right], \quad (2)$$

where $\delta = \omega_L - \omega_{13}$ is the one-photon detuning and $\omega'_L - \omega_L - \omega_{12}$ is the Raman detuning, which we will assume for simplicity to be equal to zero. The latter means that the two-photon resonance is to be broad enough to account for all the active atoms. This is possible when exciting system fields are strong enough, so that the power broadening mechanisms⁷ could overcome the residual Doppler broadening.

Adding the relaxation part of the Liouvillian to its undamped part, $\mathcal{L}_\Lambda = (i/\hbar) [\hat{\mathcal{H}}_\Lambda, \odot]$, we can rewrite the Liouvillian of the Λ -system in the form

$$\mathcal{L}_{\text{RWA}} = \begin{pmatrix} -2\gamma & \gamma & \gamma & 0 & 0 & 0 & g/\sqrt{2} & 0 & g'/\sqrt{2} \\ 0 & -\gamma_{12} & \gamma_{12} & 0 & 0 & 0 & -g/\sqrt{2} & 0 & 0 \\ 0 & w & -w & 0 & 0 & 0 & 0 & 0 & -g'/\sqrt{2} \\ 0 & 0 & 0 & -\Gamma_{12} & 0 & 0 & -g'/2 & 0 & -g/2 \\ 0 & 0 & 0 & 0 & -\Gamma_{12} & g'/2 & 0 & -g/2 & 0 \\ 0 & 0 & 0 & 0 & 0 & -g'/2 & -\Gamma & \delta & 0 \\ -g/\sqrt{2} & g/\sqrt{2} & 0 & g'/2 & 0 & -\delta & -\Gamma & 0 & 0 \\ 0 & 0 & 0 & 0 & g/2 & 0 & 0 & -\Gamma & \delta \\ -g'/\sqrt{2} & 0 & g'/\sqrt{2} & g/2 & 0 & 0 & 0 & -\delta & -\Gamma \end{pmatrix}, \quad (3)$$

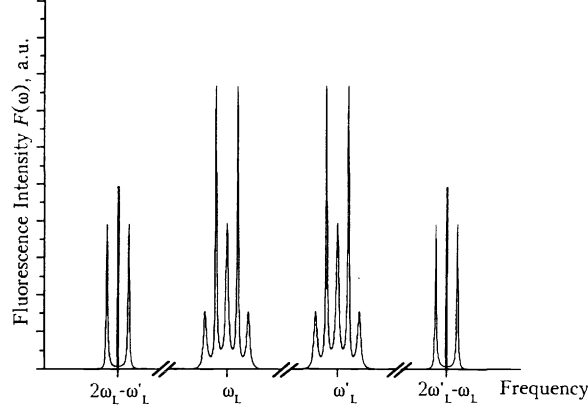


Figure 2. A schematic representation of the fluorescence spectrum of the driven Λ -system, including the four-photon spectral structures centered at the frequencies $2\omega_L - \omega'_L$ and $2\omega'_L - \omega_L$, respectively. The intensity of the four-photon spectral structures shown in the figure is magnified by a factor of two orders of magnitude to show these structures on the same graph with the regular resonance fluorescence spectrum structures centered at the laser frequencies ω_L and ω'_L .

with the use of the following basis: $\{\hat{e}_k\} = \{|3\rangle\langle 3|, |1\rangle\langle 1|, |2\rangle\langle 2|, (|1\rangle\langle 2| + |2\rangle\langle 1|)/\sqrt{2}, -i(|1\rangle\langle 2| - |2\rangle\langle 1|)/\sqrt{2}, (|1\rangle\langle 3| + |3\rangle\langle 1|)/\sqrt{2}, -i(|1\rangle\langle 3| - |3\rangle\langle 1|)/\sqrt{2}, (|2\rangle\langle 3| + |3\rangle\langle 2|)/\sqrt{2}, -i(|2\rangle\langle 3| - |3\rangle\langle 2|)/\sqrt{2}\}$. We neglected here the population relaxation rate γ_{12} and pumping rate w of the dipole forbidden transition $|1\rangle \leftrightarrow |2\rangle$.

3. CALCULATION OF THE RESONANCE FLUORESCENCE AND ABSORPTION SPECTRA

The resonance fluorescence spectrum can be calculated as Fourier transformation of the corresponding atomic correlation function^{8,9}:

$$\mathcal{K}(\tau) = \langle \hat{\rho}_0 S(0, t) [\hat{\sigma}^-(t) [S(t, t + \tau) \hat{\sigma}^+(t + \tau)]] \rangle, \quad (4)$$

where $\hat{\rho}_0$ is the initial density matrix, $\hat{\sigma}^-$ and $\hat{\sigma}^+$ are the Heisenberg transition operators, oscillating at the laser frequencies. The evolution superoperator $S(t, t + \tau)$ within the Markov approximation has the form:

$$S(t_1, t_2) = \text{T exp} \left[\int_{t_1}^{t_2} \mathcal{L}(\tau) d\tau \right],$$

where T is the symbol of the normal time ordering. If the Liouvillian parameters change much slower than the atomic relaxation rates, then the density matrix in Eq. (4) is simply given by the zero eigenvector of the Liouvillian (3). The correlation function then takes the form:

$$\mathcal{K}_{\text{RWA}}(\tau) = \sum_{k=0}^8 \left[C_k^{13} e^{(\lambda_k - i\omega_L)\tau} + C_k^{23} e^{(\lambda_k - i\omega'_L)\tau} \right] \quad (5)$$

with the intensity coefficients given by

$$C_k^{13} = \langle 0 | \hat{\sigma}_{13}^- \cdot |k\rangle \langle k | \hat{\sigma}_{13}^+, \quad C_k^{23} = \langle 0 | \hat{\sigma}_{23}^- \cdot |k\rangle \langle k | \hat{\sigma}_{23}^+, \quad (6)$$

where “ \cdot ” denotes the 3×3 -matrix multiplication; λ_k , $|k\rangle$, and $\langle k|$ are the eigenvalues, ket and bra eigenvectors of

the Liouvillian (3). Fourier transformation of the correlation function (5) gives us the fluorescence spectrum $\mathcal{F}(\omega)$:

$$\begin{aligned} \mathcal{F}(\omega) &= 2\Re e \left[\sum_{k=0}^8 \frac{C_k^{13}}{i(\omega - \omega_L) + \lambda_k} + \frac{C_k^{23}}{i(\omega - \omega'_L) + \lambda_k} \right] = \\ &2 \left[\sum_{k=0}^8 \frac{-\Re e \lambda_k \Re e C_k^{13}}{(\Re e \lambda_k)^2 + (\omega_L - \omega - \Im m \lambda_k)^2} + \frac{\Im m C_k^{13} (\omega_L - \omega - \Im m \lambda_k)}{(\Re e \lambda_k)^2 + (\omega_L - \omega - \Im m \lambda_k)^2} + \right. \\ &\left. \frac{-\Re e \lambda_k \Re e C_k^{23}}{(\Re e \lambda_k)^2 + (\omega'_L - \omega - \Im m \lambda_k)^2} + \frac{\Im m C_k^{23} (\omega'_L - \omega - \Im m \lambda_k)}{(\Re e \lambda_k)^2 + (\omega'_L - \omega - \Im m \lambda_k)^2} \right]. \end{aligned} \quad (7)$$

The probe field absorption spectra can be calculated then by analogy as the absorption probability of a photon from the weak probe field and is also determined by Fourier transformation of a superposition of certain atomic correlation functions^{1,9}:

$$P(\omega) = g_{pr}^2 A(\omega), \quad A(\omega) = \int_{-\infty}^{\infty} \mathcal{C}(\tau) e^{i\omega\tau} d\tau, \quad (8)$$

where g_{pr} is the Rabi frequency of the probe field and

$$\mathcal{C}(\tau) = \langle [\sigma^+(t) \cdot \sigma^-(t + \tau)] \rangle = \langle \sigma^+(t) \sigma^-(t + \tau) \rangle - \langle \sigma^-(t + \tau) \sigma^+(t) \rangle.$$

For the steady-state case we therefore come to the following absorption spectrum form:

$$\begin{aligned} A(\omega) &= 2g_{pr}^2 \Re e \left[\sum_{k=0}^8 \frac{D_k^{13}}{i(\omega - \omega_L) + \lambda_k} + \frac{D_k^{23}}{i(\omega - \omega'_L) + \lambda_k} \right] = \\ 2g_{pr}^2 &\left[\sum_{k=0}^8 \frac{-\Re e \lambda_k \Re e D_k^{13}}{(\Re e \lambda_k)^2 + (\omega_L - \omega - \Im m \lambda_k)^2} + \frac{\Im m D_k^{13} (\omega_L - \omega - \Im m \lambda_k)}{(\Re e \lambda_k)^2 + (\omega_L - \omega - \Im m \lambda_k)^2} + \right. \\ &\left. \frac{-\Re e \lambda_k \Re e D_k^{23}}{(\Re e \lambda_k)^2 + (\omega'_L - \omega - \Im m \lambda_k)^2} + \frac{\Im m D_k^{23} (\omega'_L - \omega - \Im m \lambda_k)}{(\Re e \lambda_k)^2 + (\omega'_L - \omega - \Im m \lambda_k)^2} \right], \end{aligned} \quad (9)$$

with the coefficients D_k^{i3} ($i = 1, 2$) given by

$$\begin{aligned} D_k^{13} &= \langle 0 | \hat{\sigma}_{13}^- \cdot |k\rangle \langle k | \hat{\sigma}_{13}^+ \rangle - \langle 0 | \hat{\sigma}_{13}^+ \cdot |k\rangle \langle k | \hat{\sigma}_{13}^- \rangle, \\ D_k^{23} &= \langle 0 | \hat{\sigma}_{23}^- \cdot |k\rangle \langle k | \hat{\sigma}_{23}^+ \rangle - \langle 0 | \hat{\sigma}_{23}^+ \cdot |k\rangle \langle k | \hat{\sigma}_{23}^- \rangle. \end{aligned} \quad (10)$$

Calculation of the resonance fluorescence spectrum due to the four-photon interactions, beyond the RWA, is much more complicated and is given in detail in Ref. 5. With an extensive use of computer algebra we were able to generalize the formula of Ref. 5 for the radiation correlation function due to the four-photon interactions (see also Eq. (4)):

$$\begin{aligned} K_{4ph}(\tau) &= \sum_{k=0}^8 \left[\frac{m_1 g^2}{4\Delta^2} \langle 0 | \hat{\sigma}_{12}^- \cdot |k\rangle \langle k | \hat{\sigma}_{12}^+ \rangle e^{-i(\omega_L - \Delta)\tau} + \right. \\ &\left. \frac{m_2 g'^2}{4\Delta^2} \langle 0 | \hat{\sigma}_{12}^+ \cdot |k\rangle \langle k | \hat{\sigma}_{12}^- \rangle e^{-i(\omega_L + \Delta)\tau} \right], \end{aligned} \quad (11)$$

where $m_1 = (\vec{e}_L \vec{d}_{23})^2 / (\vec{e}'_L \vec{d}_{23})^2$ and $m_2 = (\vec{e}'_L \vec{d}_{13})^2 / (\vec{e}_L \vec{d}_{13})^2$ characterize the efficiency of the off-resonant excitations and $\Delta = \omega'_L - \omega_L$.

From Eq. (11) one can clearly see that the novel resonance fluorescence structures are centered at the four-photon frequencies $2\omega'_L - \omega_L$ and $2\omega_L - \omega'_L$. Comparing the pre-exponential coefficients in Eq. (11) with those ones in Eq. (5) we may conclude that the four-photon resonance fluorescence structures are similar to the spectrum of oscillations of the $|1\rangle \leftrightarrow |2\rangle$ transition in the RF-range, which is, however, very weak as the transition is forbidden in dipole approximation.

4. ANALYTICAL CALCULATIONS RESULTS

To proceed with the calculations according to the Eq. (11), we need first to calculate the eigenvalues and eigenvectors of the Liouvillian (3). This, however, proves to be unfeasible unless we can apply the saturating field approximation. In this approximation we can decompose the original Liouvillian into two parts, one of which, the “unperturbed” Liouvillian, includes only the Rabi frequencies and the other one $\mathcal{L}_{\text{RWA}}|_{g=g'=0}$ can be treated as the perturbation. Then, representing the results as a series expansion for $1/g_\Lambda$, we received with the help of computer algebra the first order corrections, which generalize the zero-order results of Ref. 1. The details of our calculations are given below.

4.1. Resonance Fluorescence Spectra in the RWA

Assume for simplicity that $\Gamma_{12} \ll \Gamma$, which is easily satisfied in many cases. With this assumption the eigenvalues of the Liouvillian (3) in the first-order approximation read:

$$\begin{aligned} \lambda_0 = 0, \quad \lambda_1 = -\frac{\gamma}{2}, \quad \lambda_2 = -\Gamma, \quad \lambda_3 = ig_\Lambda - \frac{3\gamma}{4} - \frac{\Gamma}{2}, \quad \lambda_4 = -ig_\Lambda - \frac{3\gamma}{4} - \frac{\Gamma}{2}, \\ \lambda_5 = i\frac{g_\Lambda + \delta}{2} - \frac{\Gamma}{2}, \quad \lambda_6 = i\frac{g_\Lambda - \delta}{2} - \frac{\Gamma}{2}, \quad \lambda_7 = i\frac{-g_\Lambda + \delta}{2} - \frac{\Gamma}{2}, \quad \lambda_8 = i\frac{-g_\Lambda - \delta}{2} - \frac{\Gamma}{2}. \end{aligned} \quad (12)$$

The resonance fluorescence spectrum in the RWA (Eq. (5)) is determined then by the intensity coefficients (6), which are listed below:

$$\begin{aligned} C_0^{13} = C_0^{23} = C_1^{13} = C_1^{23} = 0, \quad C_2^{13} = \frac{\Gamma_{12}}{\gamma} \cos^4 \varphi \sin^2 \varphi, \quad C_2^{23} = \frac{\Gamma_{12}}{\gamma} \cos^2 \varphi \sin^4 \varphi, \\ C_3^{13} = \frac{\Gamma_{12}}{2\gamma} \cos^4 \varphi \sin^2 \varphi \left(1 + \frac{i(2\Gamma - 11\gamma)}{64g_\Lambda} \right), \quad C_4^{13} = (C_3^{13})^*, \quad C_5^{13} = C_5^{23} = 0, \\ C_3^{23} = \frac{\Gamma_{12}}{2\gamma} \cos^2 \varphi \sin^4 \varphi \left(1 + \frac{i(2\Gamma - 11\gamma)}{64g_\Lambda} \right), \quad C_4^{23} = (C_3^{23})^*, \quad C_7^{13} = C_7^{23} = 0, \\ C_6^{13} = \frac{\Gamma_{12}}{\gamma} \cos^4 \varphi \sin^2 \varphi \left(1 - \frac{i(2\Gamma - \gamma) - \delta}{g_\Lambda} \right), \quad C_6^{23} = \frac{\Gamma_{12}}{\gamma} \cos^2 \varphi \sin^4 \varphi \left(1 - \frac{i(2\Gamma - \gamma) - \delta}{g_\Lambda} \right), \\ C_8^{13} = \frac{\Gamma_{12}}{\gamma} \cos^4 \varphi \sin^2 \varphi \left(1 + \frac{i(2\Gamma - \gamma) - \delta}{g_\Lambda} \right), \quad C_8^{23} = \frac{\Gamma_{12}}{\gamma} \cos^2 \varphi \sin^4 \varphi \left(1 + \frac{i(2\Gamma - \gamma) - \delta}{g_\Lambda} \right), \end{aligned} \quad (13)$$

where $\cos \varphi = g/g_\Lambda$ and $\sin \varphi = g'/g_\Lambda$. It is important to note that the total fluorescence intensity is proportional to the ratio $\Gamma_{12}/\gamma \ll 1$, which is typically lies in the range of $10^{-2} \div 10^{-5}$ and manifests therefore the CPT in the system.

By contrast with the Mollow-triplet in the resonance fluorescence from a TLA, one can easily see from Eqs. (12) that the resonance fluorescence structures from the Λ -system consist of five incoherent lines*. If one-photon detuning δ is not equal to zero, the inner, i.e. shifted by $g_\Lambda/2$, lines acquire the additional shift $-\delta/2$ and become of unequal intensity, destroying the initial symmetry of the spectrum (Fig. 3). Thus the Λ -system proves to be more sensitive than the TLA not only to the Raman detuning, which determines the CPT resonance, but also to the one-photon detuning. The latter differs from the TLA case, where the corrections appearing due to the inexactness of the resonance are only of the second order. The five spectral lines manifest different dependencies on the fields intensity distribution determined by the parameter φ . When one field is much stronger than another one, the fluorescence of the strongly driven transition converts to the Mollow-type triplet, while the fluorescence from another driven transition has the Autler-Towns¹² structure, which consists of the two other lines of the complete spectrum (Fig. 4).

A surprising fact is that the intensity coefficients (13) are not real anymore. Their imaginary parts determine the non-lorentzian part of the spectrum (Fig. 5a), which, despite of its asymptotically small value in the saturating field limit, determines several important features of the fluorescence spectra. Namely, in the absence of elastic dephasing of the dipole allowed transitions ($\gamma = \Gamma$), the dependence of the fluorescence spectral power density for large offsets $\Delta\omega$ changes from the usual lorentzian one, $\mathcal{F}(\Delta\omega) \propto 1/\Delta\omega^2$, to a more drastic dependency, $\mathcal{F}(\Delta\omega) \propto 1/\Delta\omega^4$, as the lorentzian and non-lorentzian parts cancel one another. For the coefficients determined by Eqs. (13) the asymptote for large offsets is given by:

$$\mathcal{F}(\Delta\omega) = \frac{2\Gamma_\epsilon \Gamma_{12} \sin^2 \varphi \cos^2 \varphi}{\gamma} \frac{1}{\Delta\omega^2} + O\left(\frac{1}{\Delta\omega^4}\right), \quad (14)$$

where $\Gamma_\epsilon = \Gamma - \gamma$ is the elastic dephasing.

*In general, for the case of off-resonant excitation, resonance fluorescence structures consist of 7 spectral lines.^{10,11}

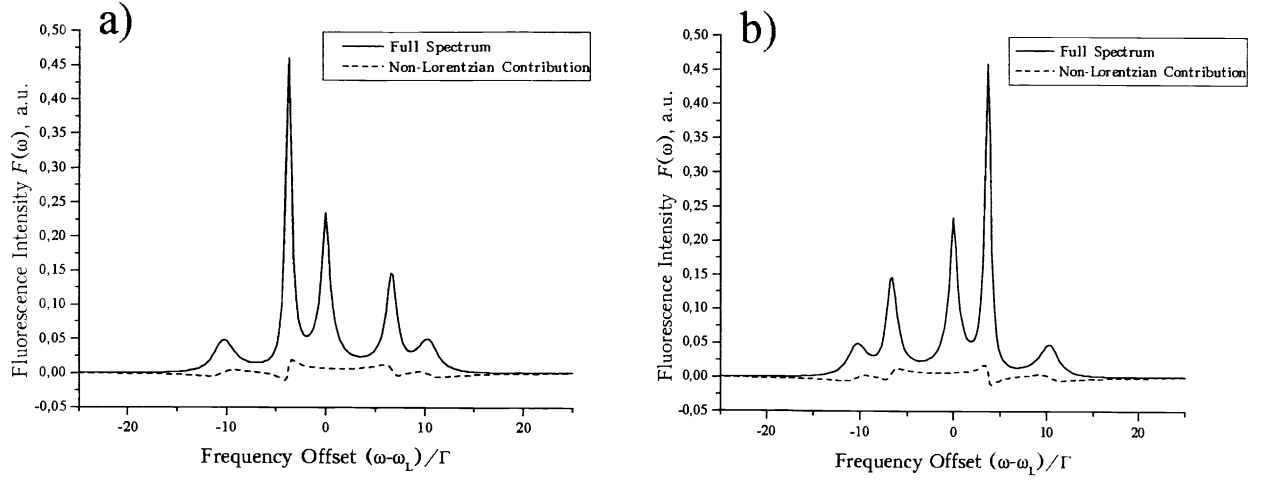


Figure 3. Fluorescence spectrum for non-zero one-photon detuning δ . The parameters used are $g_\Lambda = 10\Gamma$, $\gamma = \Gamma$, $\varphi = \pi/4$, $\Gamma_{12} = 0.001\Gamma$; $\delta = -3\Gamma$ (a), $\delta = 3\Gamma$ (b). Inner spectral lines acquire the additional frequency shift $\pm\delta/2$ and lack the intensity symmetry. Thus only the inner lines will undergo the inhomogeneous Doppler broadening if the generalized Rabi frequency g_Λ is sufficiently large, so that our theoretical model is applicable.

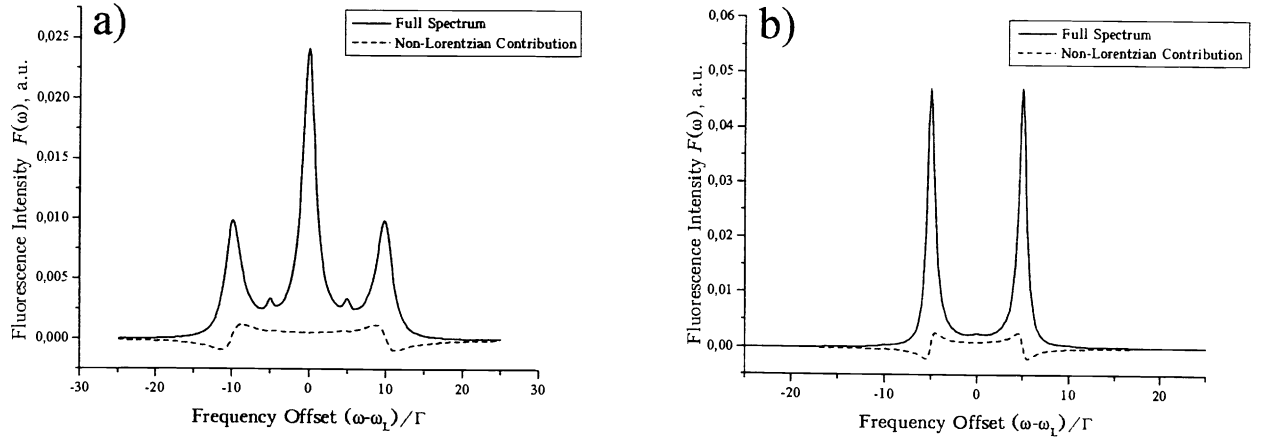


Figure 4. Resonance fluorescence spectrum in the RWA for unequal driving fields intensities (pump and probe fields, where pump field is more intensive than probe field). The fluorescence from the transition excited by pump field has a well-known Mollow-triplet structure, while the fluorescence from another transition excited by probe field exhibits Autler-Townes structure, which consists of the two remaining lines of the complete spectrum. The parameters used are $g_\Lambda = 10\Gamma$, $\gamma = \Gamma$, $\delta = 0$, $\Gamma_{12} = 0.001\Gamma$; $\varphi = \pi/20$ (a), $\varphi = 9\pi/20$ (b).

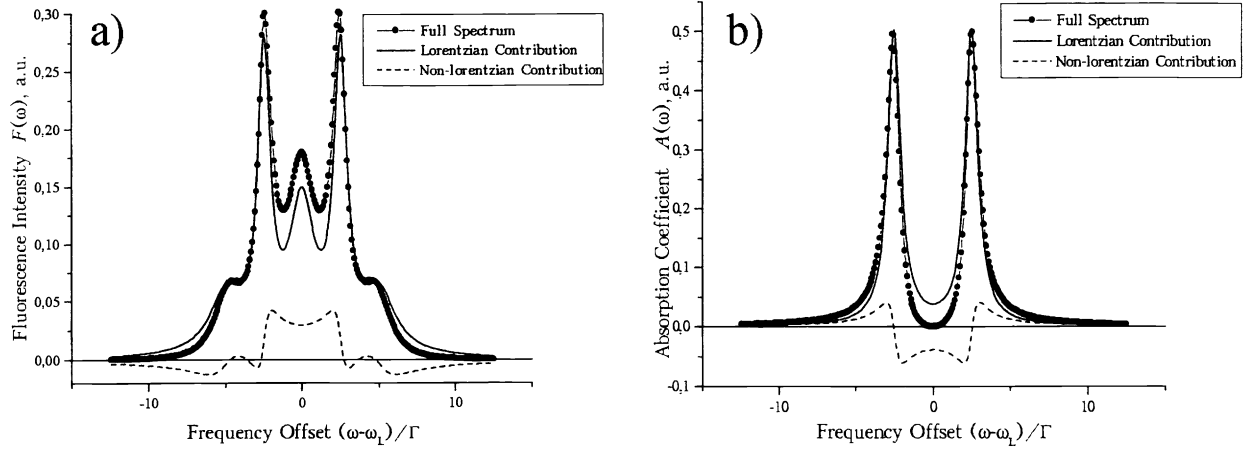


Figure 5. The resonance fluorescence (a) and probe field absorption (b) spectra of the driven Λ -system for the case of exact resonance. The spectral lines are not fully resolved here, but the non-lorentzian part reaches nearly its maximum relative value. The graphs clearly show that the non-lorentzian contribution fully compensates the lorentzian one for the cases of large offsets in the fluorescence spectrum and small offsets in the absorption spectrum. The parameters used are $g_\Lambda = 5\Gamma$, $\gamma = \Gamma$, $\varphi = \pi/4$, $\delta = 0$, $\Gamma_{12} = 0.001\Gamma$.

4.2. Probe Field Absorption Spectra

Calculation of the probe field absorption spectrum (Eq. (9)) can be done by analogy with the calculation of the fluorescence spectrum and one can readily find that among the coefficients (10), which determines the absorption spectrum, only the following coefficients are non-zero ones:

$$\begin{aligned} D_5^{13} &= \frac{1}{2} \sin^2 \varphi \left(1 + \frac{i\Gamma + \delta}{g_\Lambda} \right), & D_5^{23} &= \frac{1}{2} \cos^2 \varphi \left(1 + \frac{i\Gamma + \delta}{g_\Lambda} \right), \\ D_7^{13} &= \frac{1}{2} \sin^2 \varphi \left(1 - \frac{i\Gamma + \delta}{g_\Lambda} \right), & D_7^{23} &= \frac{1}{2} \cos^2 \varphi \left(1 - \frac{i\Gamma + \delta}{g_\Lambda} \right). \end{aligned} \quad (15)$$

This means that the probe field absorption spectrum structures consist of only two lines shifted by $\pm g_\Lambda/2$ from the laser frequencies (Fig. 5b). The inexactness of the resonance will also lead to the additional shift of the lines $\delta/2$, but in the opposite direction. The non-lorentzian part here plays an important role once again. In the absorption spectra the non-lorentzian part compensates the lorentzian one for the small offsets, so that the absorption is practically vanished at the laser frequencies, which is just another manifestation of the CPT, the self-induced transparency.⁴

4.3. Resonance Fluorescence Spectra due to the Four-Photon Interactions

The fluorescence structures due to the four-photon interactions are determined by the following coefficients in Eq. (11):

$$\begin{aligned} C_0^{lf} &= \frac{m_1 g_\Lambda^2}{4\Delta^2} \cos^4 \varphi \sin^2 \varphi, & C_0^{hf} &= \frac{m_2 g_\Lambda^2}{4\Delta^2} \cos^2 \varphi \sin^4 \varphi, \\ C_5^{lf} &= \frac{m_1 g_\Lambda^2}{8\Delta^2} \cos^2 \varphi \sin^4 \varphi \left(1 - \frac{i\Gamma + \delta}{g_\Lambda} \right), & C_5^{hf} &= \frac{m_2 g_\Lambda^2}{8\Delta^2} \cos^4 \varphi \sin^2 \varphi \left(1 + \frac{i\Gamma + \delta}{g_\Lambda} \right), \\ C_7^{lf} &= \frac{m_1 g_\Lambda^2}{8\Delta^2} \cos^2 \varphi \sin^4 \varphi \left(1 + \frac{i\Gamma + \delta}{g_\Lambda} \right), & C_7^{hf} &= \frac{m_2 g_\Lambda^2}{8\Delta^2} \cos^4 \varphi \sin^2 \varphi \left(1 - \frac{i\Gamma + \delta}{g_\Lambda} \right), \end{aligned} \quad (16)$$

the rest of them being equal to zero.

The fluorescence spectrum due to the four-photon interactions consists of two spectral structures centered at the four-photon frequencies $2\omega_L - \omega'_L$ and $2\omega'_L - \omega_L$, respectively. Each of these structures consists of a coherent and two broadened lines, which have the same shape as the broadened lines in the absorption spectra (Fig. 6). The

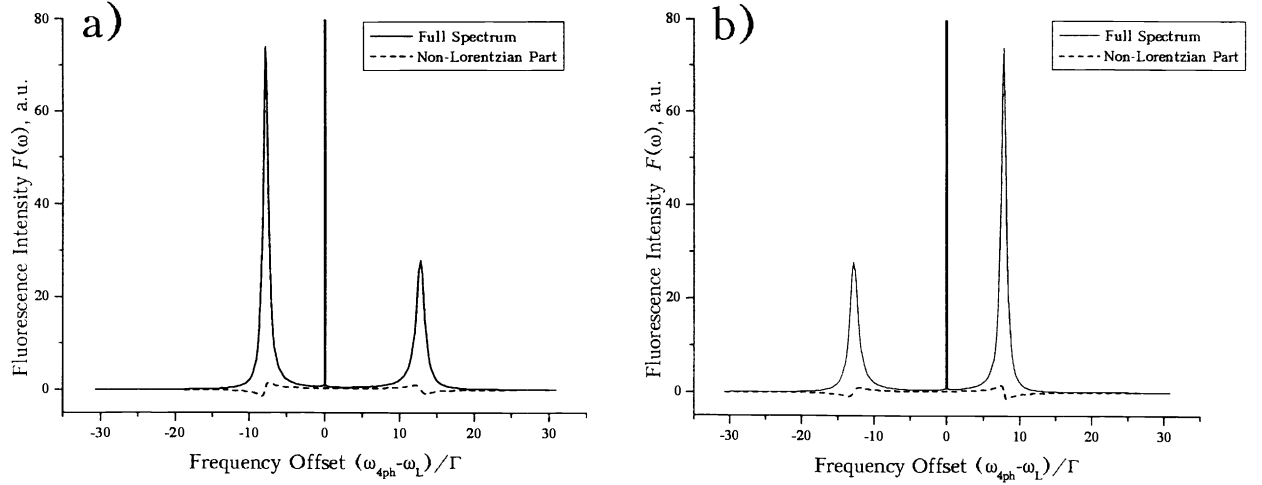


Figure 6. The fluorescence structures due to the four-photon interactions for the case of non-zero one-photon detuning δ . The broadened spectral lines acquire additional shift $\pm\delta/2$; their intensities are also different. These graphs, except for the coherent line, are absolutely identical to those of the absorption spectra in the case of inexact resonance. The parameters used are $g_\Lambda = 20\Gamma$, $\gamma = \Gamma$, $\varphi = \pi/4$, $\Gamma_{12} = 0.001\Gamma$; $\delta = 5\Gamma$ (a), $\delta = -5\Gamma$ (b).

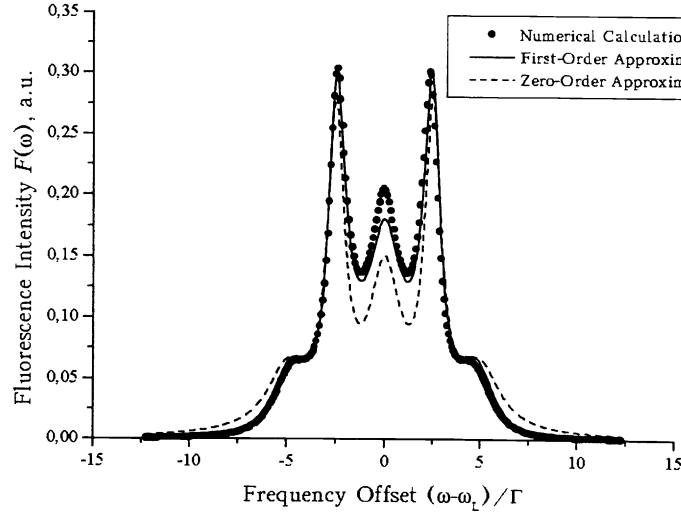


Figure 7. Comparison between numerical and approximate analytical calculations. Taking into account the first order corrections, we obtain a very good agreement with the results of the numerical calculations, even if the condition $g_\Lambda \gg \Gamma$ is not very well satisfied. The parameters used are $g_\Lambda = 5\Gamma$, $\gamma = \Gamma$, $\varphi = \pi/4$, $\delta = 0$, $\Gamma_{12} = 0.001\Gamma$.

four-photon fluorescence does not saturate, its intensity grows with the increasing strength of the driving fields as long as the condition $g_\Lambda \ll \Delta$ is satisfied and Eq. (11) received in Ref. 5 is valid. If g_Λ is large enough, the four-photon fluorescence may be strong enough to be experimentally observed and even may be stronger than the conventional RWA fluorescence, which vanishes under the CPT condition.

5. CONCLUSIONS

In this paper we obtained a novel contribution to both the resonance fluorescence and weak probe field absorption spectra of the driven Λ -system. This contribution is due to the first order corrections in the saturating field limit approximation. With an extensive use of computer algebra we received analytical formulae, which are in good agreement with the numerical calculations (Fig. 7). Analyzing our analytical results we revealed some new properties of the spectra. In our first-order approximation model only the inner lines acquire an additional shift in the case of inexact resonance, making them more sensitive to the Doppler broadening. The non-lorentzian part, though small under given approximations, strongly modifies the behavior of the fluorescence spectra for large offsets and absorption spectra for the small ones.

The four-photon interaction processes cause appearance of the four-photon resonance fluorescence structures centered at the four-photon frequencies $2\omega'_L - \omega_L$ and $2\omega'_L - \omega_L$. Their spectrum, calculated to the first-order corrections to the RWA, consists of a coherent and two broadened lines and has the same structure as the oscillations in the RF-range, corresponding to the transition between the two lower levels, but is more easily observed in the optical range of frequencies.

ACKNOWLEDGMENTS

This work was supported by Volkswagen-Stiftung (grant No. 1/72944) and by the Russian Foundation for Basic Research (grant No. 96-03-32867). V. N. Z. also thanks the Alexander von Humboldt foundation for its support.

REFERENCES

1. A. S. Manka, H. M. Doss, L. M. Narducci, R. Pu, and J. L. Oppo *Phys. Rev. A* **43**, p. 3749, 1991.
2. W. H. Louisell, *Quantum Statistical Properties of Radiation*, Wiley, New York, 1990.
3. L. Mandel and E. Wolf, *Optical Coherence and Quantum Optics*, Cambridge, New York, 1995.
4. E. Arimondo, "Coherent population trapping in laser spectroscopy." *Progress in Optics* **35**, pp. 257-354, 1996.
5. B. A. Grishanin, V. N. Zadkov, and D. Meschede *J. of Exp. and Theor. Phys. (JETP)* **113**, p. 144, 1998.
6. B. A. Grishanin, V. N. Zadkov, and D. Meschede *Phys. Rev. A* . (in print).
7. P. L. Kelley, P. J. Harshman, O. Blum, and T. K. Gustafson *J. Opt. Soc. Am. B* **11**, p. 2298, 1994.
8. B. R. Mollow *Phys. Rev.* **188**, p. 1969, 1969.
9. B. R. Mollow *Phys. Rev. A* **5**, p. 2217, 1972.
10. C. Cohen-Tannoudji and S. Reynaud *J. Phys. B* **10**, p. 345, 1977.
11. C. Cohen-Tannoudji and S. Reynaud *J. Phys. B* **10**, p. 2311, 1977.
12. S. H. Autler and C. H. Towns *Phys. Rev.* **100**, p. 703, 1969.